Obsidian pyroclasts in the Yellowstone-Snake River Plain ignimbrites are dominantly juvenile in origin

Bulletin of Volcanology (2021) 83: 27
https://doi.org/10.1007/s00445-021-01448-1

RESEARCH ARTICLE

Obsidian pyroclasts in the Yellowstone-Snake River Plain ignimbrites are dominantly juvenile in origin

L. R. Monnereau[1] · B. S. Ellis[1] · D. Szymanowski[2] · O. Bachmann[1] · M. Guillong[1]

Received: 11 December 2020 / Accepted: 3 March 2021 / Published online: 29 March 2021

Abstract
Dense, glassy pyroclasts found in products of explosive eruptions are commonly employed to investigate volcanic conduit processes through measurement of their volatile inventories. This approach rests upon the tacit assumption that the obsidian clasts are juvenile, that is, genetically related to the erupting magma. Pyroclastic deposits within the Yellowstone-Snake River Plain province almost without exception contain dense, glassy clasts, previously interpreted as hyaloclastite, while other lithologies, including crystallised rhyolite, are extremely rare. We investigate the origin of these dense, glassy clasts from a coupled geochemical and textural perspective combining literature data and case studies from Cougar Point Tuff XIII, Wolverine Creek Tuff, and Mesa Falls Tuff spanning 10 My of silicic volcanism. These results indicate that the trace elemental compositions of the dense glasses mostly overlap with the vesiculated component of each deposit, while being distinct from nearby units, thus indicating that dense glasses are juvenile. Textural complexity of the dense clasts varies across our examples. Cougar Point Tuff XIII contains a remarkable diversity of clast appearances with the same glass composition including obsidian-within-obsidian clasts. Mesa Falls Tuff contains clasts with the same glass compositions but with stark variations in phenocryst content (0 to 45%). Cumulatively, our results support a model where most dense, glassy clasts reflect conduit material that passed through multiple cycles of fracturing and sintering with concurrent mixing of glass and various crystal components. This is in contrast to previous interpretations of these clasts as entrained hyaloclastite and relaxes the requirement for water-magma interaction within the eruptive centres of the Yellowstone-Snake River Plain province.

Keywords Yellowstone-snake river plain · Obsidian · Pyroclastic · Trace elemental geochemistry

Introduction

Volatile elements (predominantly H, C, S, and Cl) are a primary control on many magmatic and volcanic processes. Of particular relevance is the potential for variations in these volatile components of magmas to drive changes in eruptive style. These changes from hazardous explosivity to more benign effusive activity may occur over the history of a volcano, with successive eruptions having different style, or may occur within a single eruption (Christiansen 2001; Cassidy et al. 2018). Estimating the pre-eruptive volatile budget of a magma may be carried out through the use of mineral-melt hygrometry (Waters and Lange 2015). While providing important information about the pre-eruptive state of the magma, the hygrometry approach is limited by the fact that it only informs about the water content and that it requires an accurate and precise estimate of the temperature of the magma prior to eruption. An alternative approach is to measure the volatile contents of melt inclusions which allows direct measurement of a variety of volatile components. The volatile inventories returned by analysis of melt inclusions are known to be potentially compromised by diffusion of elements through the host crystal (Portnyagin et al. 2008; Lloyd et al. 2013), formation of bubbles within the inclusion (e.g. Moore et al. 2015; Wallace et al. 2015; Rasmussen et al. 2020; amongst others), and post-entrapment crystallisation.

Challenges determining the pre-eruptive volatile content of the magma are compounded by the fact that many of the important controls on gas retention within a magma

Editorial responsibility: A.V. Ivanov

L. R. Monnereau
lmonnereau@student.ethz.ch

[1] Institute of Geochemistry and Petrology, ETH Zürich, 8092 Zurich, Switzerland

[2] Department of Geosciences, Princeton University, Princeton, NJ 08544, USA

(e.g. permeability and porosity of the magma) may change within the conduit on short (hours to minutes) timescales (Humphreys et al. 2008). With melt inclusions typically not thought to be entrapped within the conduit, alternative sources of information must be sought to quantify these crucial changes. Some studies have focussed on the most rapid diffusers (typically H or Li) in either mineral phases (Jollands et al. 2020) or melt embayments (Myers et al. 2016) and such techniques hold considerable promise. Other studies have looked at the melt behaviour as a whole (i.e. away from crystal phases) investigating how repeated cycles of fracturing and sintering may act as a mechanism to periodically release gas from the magma and control explosivity (Castro et al. 2014; Schipper et al. 2021). Many of these studies have focussed on the volatile contents of dense, glassy pyroclasts to infer the degassing behaviour of the magma within the conduit. The identity of such obsidian clasts is the topic of this study.

Obsidian pyroclasts

The term 'pyroclastic' is derived from the Greek *pur*, meaning 'fire' and *klastos*, meaning 'broken pieces' and refers to clastic or fragmentary material resulting from explosive phenomena (Froggatt and Lowe 1990), which may or may not have a genetic link with the co-erupting juvenile component of the eruption. In addition to the vesiculated fragments formed during explosive volcanism, dense, poorly vesiculated volcanic glass is also often ejected. These dense glass clasts are often loosely termed 'obsidian' as many of the fragments are sufficiently small to preclude determining whether the original glassy source material contained phenocrysts (i.e. was vitrophyric) or not (i.e. a true obsidian). Here we also use the term 'obsidian' to refer to dense glass regardless of the content of large crystals.

Obsidian pyroclasts are a common feature of many silicic pyroclastic deposits such as the P series tephra at Sete Cidades (Queiroz et al. 2008); Panum Crater (Fink 1987), Newberry (Rust and Cashman 2007), and Bishop Tuff (Hildreth and Mahood 1986) amongst many other examples (Supplementary Table 1). These obsidians have been used to address the volatile evolution of the magma within the difficult to access conduit region. Studies of obsidians have predominantly focussed on magmatic degassing using a variety of approaches, including the water and CO_2 systematics (Newman et al. 1988; Dunbar and Kyle 1992; Watkins et al. 2017; Gardner et al. 2017), water contents and hydrogen isotopes (Taylor et al. 1983; Newman et al. 1988; Rust et al. 2004), and chlorine contents and isotopes (Barnes et al. 2014). These studies, and others, have proposed a range of conduit behaviours for ascending magma, from approximating a closed-system (Newman et al. 1988), to continuous vapour buffering through permeable margins (Rust et al. 2004), to ephemeral permeability of the magma and conduit due to various fracturing and agglutination processes (Cabrera et al. 2011; Gardner et al. 2017; Watkins et al. 2017; Wadsworth et al. 2020; Wang et al. 2021).

It is implicit within these models that the obsidian clasts being studied are genetically linked to the juvenile magma erupting, and so findings from the obsidian clasts can be applied to the dynamics of the eruption in question. However, often a rigorous demonstration of this linkage is absent. Compositional 'fingerprinting' of pyroclast populations is thus fundamental to ensuring that obsidians (and so any information about volatile inventories that is derived from them) are genetically related to the eruption deposits they are found within. These compositional methods must be sufficiently sensitive to be able to discriminate between successive magma batches from a single volcanic centre. This study combines textural and compositional information from both obsidians and juvenile components of ignimbrites from the Snake River Plain-Yellowstone magmatic province to investigate the origin of obsidian clasts.

The Yellowstone-Snake River Plain (YSRP) province

The Columbia River–Snake River Plain–Yellowstone is a large igneous province (LIP) in northwest USA, extending from Nevada-Oregon to Wyoming. Since the mid-Miocene, it has been associated with broadly bimodal (basalt–rhyolite) volcanism. Silicic activity related to this province was initially widely dispersed prior to narrowing to a broadly time-transgressive pattern of activity with eruptive centres younging to the north-east with current activity at the Yellowstone volcanic field. Silicic volcanism in the central Snake River Plain has an association of lithofacies sufficiently different from other rhyolitic systems to be considered by Branney et al. (2008) as a distinct category of volcanic activity, 'Snake River-type volcanism'. As relevant to this study, the ignimbrites associated with SR-type volcanism are produced from hot, dry magmas and exhibit a bimodality of welding intensity, with most ignimbrites intensely welded while a minority are non-welded. Eutaxitic, moderately welded ignimbrites as characterise many other settings are rare to absent. Ignimbrites in the central Snake River Plain typically contain few if any discernible pumice or lithic clasts but upon passing both east and west the intensity of the SR-type character decreases and ignimbrites show more pumice and lithic clasts. Common throughout all of the ignimbrites of the YSRP (and indeed, globally) are small (typically mm to cm-scale) sub-angular clasts of dense obsidian and vitrophyre. From the central Snake River Plain, such dense glassy clasts have been reported from the Magpie Basin, Cougar Point Tuff XIII, Steer Basin, Wooden Shoe Butte, Little Creek, Dry Gulch, McMullen Creek, Castleford Crossing, Brown's Bench, Brown's View, and Sand Springs units (Andrews et al. 2008; Ellis et al. 2010; Ellis and Branney 2010; Knott et al. 2016a, b). At the Heise centre, they are known from the Wolverine Creek and Kilgore Tuff units (Ellis et al. 2017) and at Yellowstone they occur within the Huckleberry Ridge, Mesa Falls, Sulphur Creek, and Uncle Tom's Trail deposits (Pritchard and Larson 2012; Myers et al. 2016; Swallow et al. 2018). Examples of these glassy clasts are illustrated in Fig. 1.

Previous studies (Branney et al. 2008) have interpreted these dense, glassy clasts as hyaloclastite formed within the caldera and then entrained into subsequent explosive eruptions. Under this scenario, the dense glassy clasts are lithics and unrelated to the erupted magma. In this study, we use trace element geochemistry to characterise the obsidian clasts and compare them to the vesicular juvenile components of the eruption with three main case studies described below, with their relative locations shown in Fig. 2.

1) Mesa Falls Tuff, Yellowstone Volcanic Field, ID-WY, USA:

   The 1.3 Ma rhyolitic Mesa Fall Tuff (MFT), erupted from the Henry's Fork caldera, is the second of the three Yellowstone caldera-forming eruptions, each preceded and followed by rhyolitic flows (Christiansen 2001). This eruption produced ~ 280 km^3 of ignimbrite over ~ 2700 km^2 during Pleistocene and is interpreted as a single and simple eruptive unit (Fig. 2). The deposit is commonly 30–70 m thick, but reaches a maximum of 150 m. With its pinkish colour, it is characterised by abundant large phenocrysts (especially sanidine and quartz), contains welded and non-welded lithologies, and is relatively lithic-poor. The base of the unit is a thick-bedded ash and pumice layer with dense glass chips (sampled for this study), well sorted, with a dominant white colour.

2) Cougar Point Tuff XIII, central Snake River Plain, ID-NV, USA:

   The enormous volume (1470 km^3) Cougar Point Tuff XIII rhyolite (CPT XIII) covers an area of at least 24,500 km^2 in the central Snake River Plain (Fig. 2) with high-precision ID-TIMS zircon ages defining that the eruption occurred at 11.030 ± 0.006 Ma (Ellis et al. 2019). Variably exposed CPT XIII fallout deposits are found south of the Snake River Plain in the Cassia Mountains and Bruneau-Jarbidge regions. Overlying the metre-scale fallout deposits is a thick, typically intensely welded ignimbrite of moderate (c. 10%) crystallinity. Glassy chips have been reported from a number of locations within the ignimbrite of CPT XIII, in the Cassia Mountains (Ellis et al. 2010), south of the town of Jackpot, NV (Andrews et al. 2008; Knott et al. 2016b) and here we use a sample from the north-eastern portion of the deposit in the East Bennett Mountains (a portion of the deposit previously referred to as the Tuff of Fir Grove).

3) Wolverine Creek Tuff, eastern Snake River Plain, ID, USA:

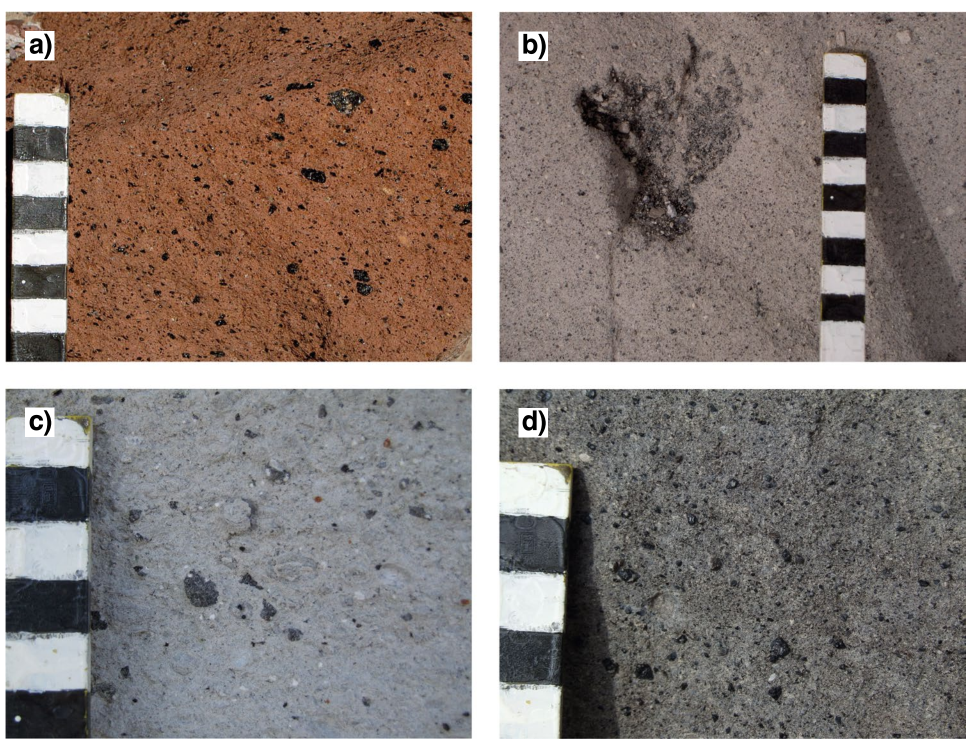

Fig. 1 Field images of examples of the dense glass clasts within ignimbrites of the Yellowstone-Snake River Plain province. Divisions on ruler in all cases are 1 cm. **a** Dense glass pieces sitting within pink 'Jackpot 6′ deposit directly overlying Cougar Point Tuff XIII south of the town of Jackpot, NV (Andrews et al. 2008). **b** Plan view of elutriation pipe in the Wolverine Creek Tuff with the dark colour resulting from a predominance of dense obsidian clasts. **c** Multiple dense glass clasts within the non-welded Deadeye Member of Ellis and Branney (2010) in the Cassia Mountains. **d** Non-welded basal portion of the Tuff of Wooden Shoe Butte from Trapper Creek containing abundant small obsidian clasts (Knott et al. 2016b)

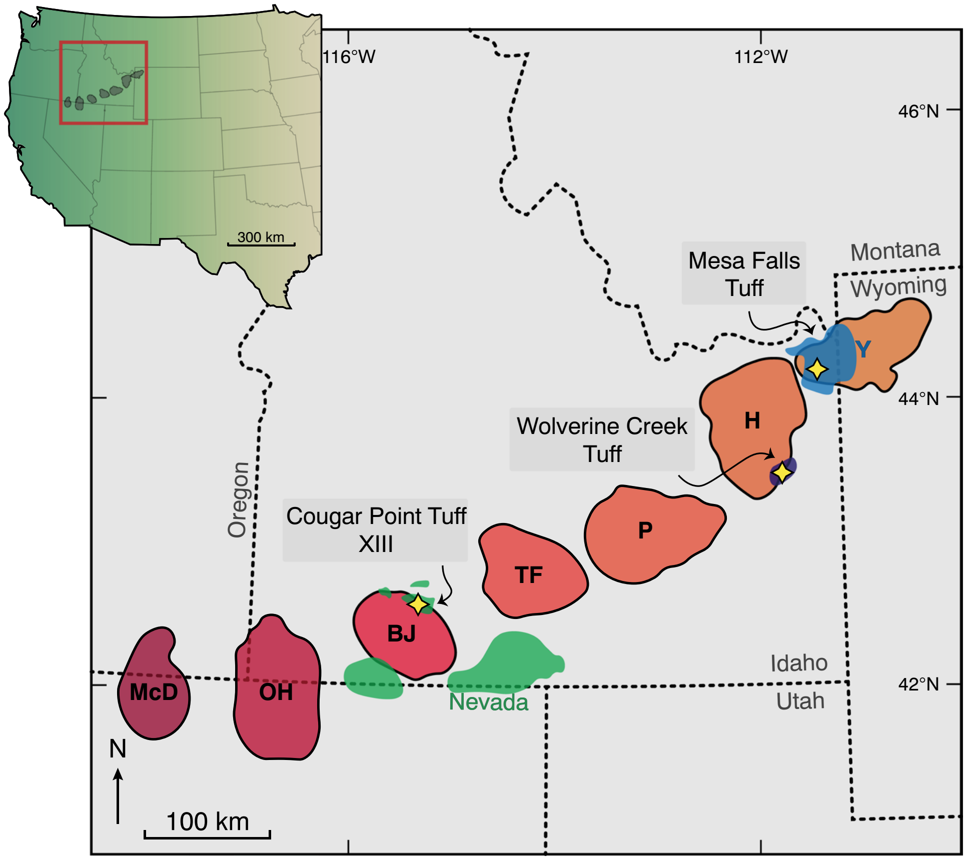

Fig. 2 Overview location map showing the CPT XIII, Wolverine Creek Tuff, and Mesa Falls Tuff with sampling sites (yellow stars) that serve as examples in this study. Abbreviations of the eruptive centres from the Yellowstone–Snake River Plain volcanic province are: McD—McDermitt; OH—Owyhee Humboldt; BJ—Bruneau–Jarbidge; TF—Twin Falls; P—Picabo; H—Heise; Y—Yellowstone

The Heise volcanic field, active between c. 6.6 and 4 Ma in the eastern Snake River Plain, produced a number of large-volume rhyolitic ignimbrites that are typically welded. At 5.5941 ± 0.0097 Ma, the physically distinct, but temporally and petrographically related Conant Creek and Wolverine Creek tuffs (CCT and WCT) were erupted (Szymanowski et al. 2016). The Wolverine Creek Tuff is entirely non-welded and contains 4 distinct morphologies of volcanic glass (Fig. 3): microvesicular pumice clasts, macrovesicular elongate shards, macrovesicular classic SR-shards, and dense angular to sub-rounded chips of dense black glass (Szymanowski et al. 2015). The dense glass clasts are particularly abundant within, and often act to pick out, elutriation pipes within the deposit where the less dense, vesicular, glass morphologies have been preferentially removed by gas escaping from the recently deposited ignimbrite (see Fig. 1b, also Fig. 5.5D of Branney and Kokelaar 2002).

Methods

Images of the obsidians in thin sections and mounts were obtained using a polarising microscope and back-scattered electron microscopy (FEI Quanta 200 FEG scanning electron microscope, with 10 kV accelerating voltage). Trace element analyses of individual glass fragments from the three case studies were performed via laser ablation inductively coupled plasma mass spectrometry (LA-ICPMS) at the Institute of Geochemistry and Petrology, ETH Zürich. For drift correction, the NIST-612 silicate glass reference material was measured twice after every 20–30 unknowns, with GSD-1G and ATHO-G (one measurement for each per batch) glasses used to monitor performance. For the data reduction, the averages of SiO_2 content in glass and groundmass were used as an internal standard—77% and 76% SiO_2 for MFT (from supplementary data from Neukampf et al. 2019) and CPT XIII, respectively. The element concentrations were calculated with the MATLAB-based program SILLS (Guillong et al. 2008), and three spot analyses were performed on each fragment, giving a precision better than 5% for elements that are appreciably above the limits of detection. All new analyses and standard measurements are provided in supplementary material. For the MFT samples, phenocryst contents of dense glassy clasts were estimated using the ImageJ software using the surfaces of clasts exposed within the epoxy mount and measuring total exposed area and exposed area of crystal phases.

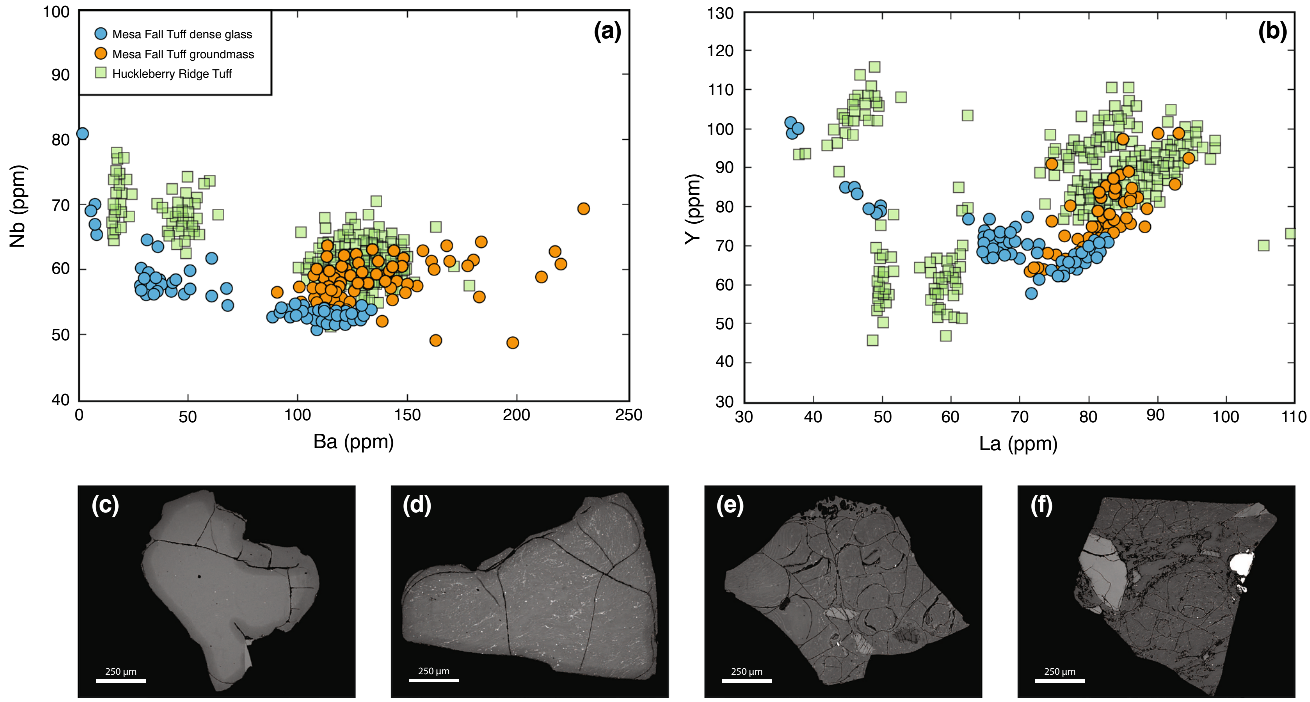

Fig. 3 Composition and appearance of obsidian clasts within Mesa Falls Tuff. **a**, **b** Trace elemental compositions of MFT obsidian clasts compared to MFT juvenile compositions (Neukampf et al. 2019) with additional Yellowstone data from Swallow et al. 2018 shown for comparison. **c**–**f** Variations in the appearance of the dense glass clasts in the MFT

Results

Mesa Falls Tuff

Backscattered electron images (Fig. 3c–f) reveal that the dense glass clasts within the MFT show considerable variability in appearance (a gallery of images available in Supplementary Fig. 2). A first-order difference between the dense glass clasts is the presence or absence of phenocrysts. These crystals are typically quartz or sanidine that are the main mineral phases occurring with the Mesa Falls Tuff (and indeed virtually all Yellowstone rhyolites). The glass chips are typically a few millimetres in diameter and range from having phenocryst proportions of zero (e.g. c and d in Fig. 3) up to 45%. Other textural features of the obsidians appear to only be weakly related to the presence or absence of large crystals. Some of the obsidians show evidence for incipient devitrification with small patches of felty intergrowths of quartz and sanidine occurring at point sources and radiating outwards. Small trails of Fe-Ti oxides are found within the dense glasses producing a flow-banded effect; many of these trails may be highlighting the margins of former shards within the now dense glass. Superimposed on these textural variations are numerous perlitic cracks that may contain regions of brighter backscatter response and vary from pervasive to absent between clasts.

Obsidian pyroclasts from the Mesa Falls Tuff show a large range of trace element compositions with many compositions distinct from those in the vesiculated pumice glass. One compositional cluster, with Nb between 51 and 57 ppm and Ba of 88–133 ppm, is nearly identical to vesiculated groundmass glasses (Fig. 4a). The other obsidian compositions extend to higher Nb and lower Ba concentrations (in the ranges of ~55–90 ppm and ~1–70 ppm), readily distinguishing them from the juvenile component of the eruption. The slight difference between the majority of obsidian clasts and the groundmass glass observed in the MFT may be a function of slight zonation within the deposit, or a relatively small number ($N = 59$) of analysed samples (both obsidians and groundmass glasses coming from the same sample). Alternatively, the subtle differences may be day-to-day variability in instrumental performance as the samples were analysed in different analytical sessions. Recalculating the Neukampf et al. (2019) GSD-1G reference material data to the same internal standard used here results in the GSD-1G values being between 1 and 4% higher in the Neukampf dataset. In the case of the Huckleberry Ridge Tuff (Fig. 3a and b; Myers et al. 2016), it is notable that the compositional spread of the glasses is greater from a greater number of samples ($N = 189$). Within the MFT, there is no relationship between the phenocryst content of the dense glassy clast and the composition of the glass within the clast.

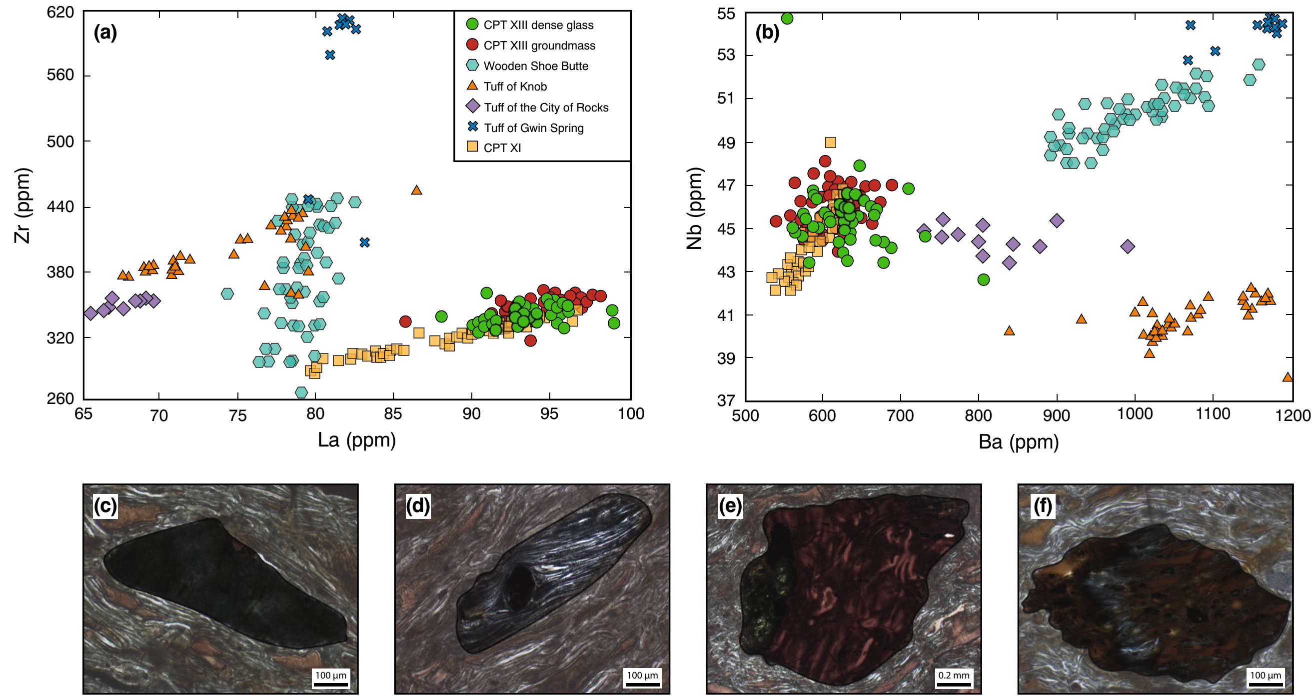

Fig. 4 Composition and appearance of obsidian clasts within Cougar Point Tuff XIII. **a**, **b** Trace elemental abundances showing the overlap between obsidians and groundmass in CPT XIII while other rhyolites of the CSRP have distinctly different compositions (additional data from Ellis et al. 2018 and Neukampf et al. 2019). **c**–**f** Variability in the appearance of the obsidian clasts. Notably the shards in the groundmass of the ignimbrite are deformed around the obsidian clasts and the flow banding within the obsidians commonly opposes that within the groundmass indicating the clasts were already solidified prior to transport and emplacement

Cougar Point Tuff XIII

The welded nature of CPT XIII allows the obsidian clasts to be characterised within thin section, revealing their relationship with the surrounding groundmass (Fig. 4). The obsidian clasts in CPT XIII show a remarkable variability in appearance, with a few common clast types distinguishable. The first is mostly dark or greyish, microlite-rich, and typically homogeneous within a clast (Fig. 4c); the second is microlite-poor, with brownish and greyish well-defined flow bands of alternating brightness (Fig. 4d); and the third type is characterised by its brown or dark reddish tinge, and irregular flow banding (Fig. 4e). Other, less common, obsidians are more complex: they contain bubbles (slightly flattened) and have a strong irregularly shaped flow banding, with some brown and grey zones (Fig. 4f). Within some dense clasts, there even exists appreciable stratigraphy with a distinct obsidian clast found within another obsidian clast. This micro-scale stratigraphy indicates that the processes of fracturing and sintering such obsidians are repetitive as suggested in other studies (e.g. Gardner et al. 2017; Watkins et al. 2017; Wadsworth et al. 2020; Wang et al. 2021). An important feature of the dense glass clasts within CPT XIII is that they are randomly orientated with respect to the welding fabric preserved by the flattened glass shards in the groundmass. In addition, the obsidian clasts remain undeformed despite their rhyolitic compositions and thus we consider that they were cold (or sufficiently cold to remain rigid) at the time of deposition.

The compositions of the dense glasses in CPT XIII are almost identical to the groundmass glass with La contents of ~86–99 ppm, Zr contents of ~318–364 ppm, Ba of ~541–709 ppm, and Nb contents of 43–48 ppm (Fig. 4a and b). The low Ba contents of Cougar Point tuffs XI and XIII glasses (Fig. 4) result from these units containing appreciable sanidine while the other ignimbrites contain only trace sanidine (e.g. Tuff of Knob) or lack it entirely (Tuff of City of Rocks). The REE patterns of the CPT XIII glasses are typical for Snake River Plain ignimbrites (see Fig. 6 in Supplementary material), and Eu/Eu* anomalies defined as ($Eu/Eu^* = Eu_N/(Sm_N.Gd_N)^{0.5}$) where $_N$ denotes chondrite-normalised abundance (McDonough and Sun 1995) are mostly between 0.22 and 0.27. Despite the remarkably variable appearance of the obsidians in thin section, only a few of them have compositions that are distinct from the individual, flattened glass shards in the welded matrix.

Wolverine Creek Tuff

The dense glass clasts of the Wolverine Creek Tuff (WCT) show little variability in appearance from clast to clast. These clasts typically have rounded outer margins and lack phenocrysts (Fig. 5). They do contain Fe-Ti oxide microlites with textures varying from random to subtly flow banded. A notable feature of the WCT glass clasts is the common occurrence of variability in backscattered electron brightness with the rims systematically darker than the cores. Often these clast margins are cut by cracks that do not pass into the backscatter bright interior and are interpreted as reflecting the hydration of the clast. The vesicular portions of the WCT deposits are variably microvesicular pumice or large, thick-walled shards with outlines reflecting the former presence of bubbles. These glasses, by contrast, do not exhibit the variations in backscattered electron brightness observed in the dense clasts (Fig. 5).

Compositionally, the dense glass fragments from the WCT are identical to the vesicular portions of the same deposit (Fig. 5a and b). Moreover, all of the WCT compositions are distinct from the other glass compositions produced during Heise volcanism with higher Nb and Y contents of ~58–60 ppm and ~62–65 ppm (Fig. 5). We highlight here that Fig. 5 even includes the glass compositions from the younger Kilgore Tuff (Ellis et al. 2017). While such compositions had not yet been produced, and so were unavailable to be sampled during the WCT eruption, they further highlight the distinctive nature of the WCT glasses at Heise and the ability of trace elemental geochemistry to distinguish juvenile components that can act as a comparison for obsidians.

Discussion

The utility of trace elements

Tephrochronology is built upon the ability to discriminate tephra samples (typically done via glass compositions) and provide a stratigraphic framework that can be placed in an absolute timeframe (review by Shane 2000). This can be done by using either major or trace elemental compositions of the glasses. In this study, we illustrate the utility of trace element measurements for this purpose as they are more sensitive to the processes of assimilation and crystallisation than the major elements. For example, in rhyolitic melts Ba may have a dynamic range of two orders of magnitude while major elements typically vary by much less (depending on

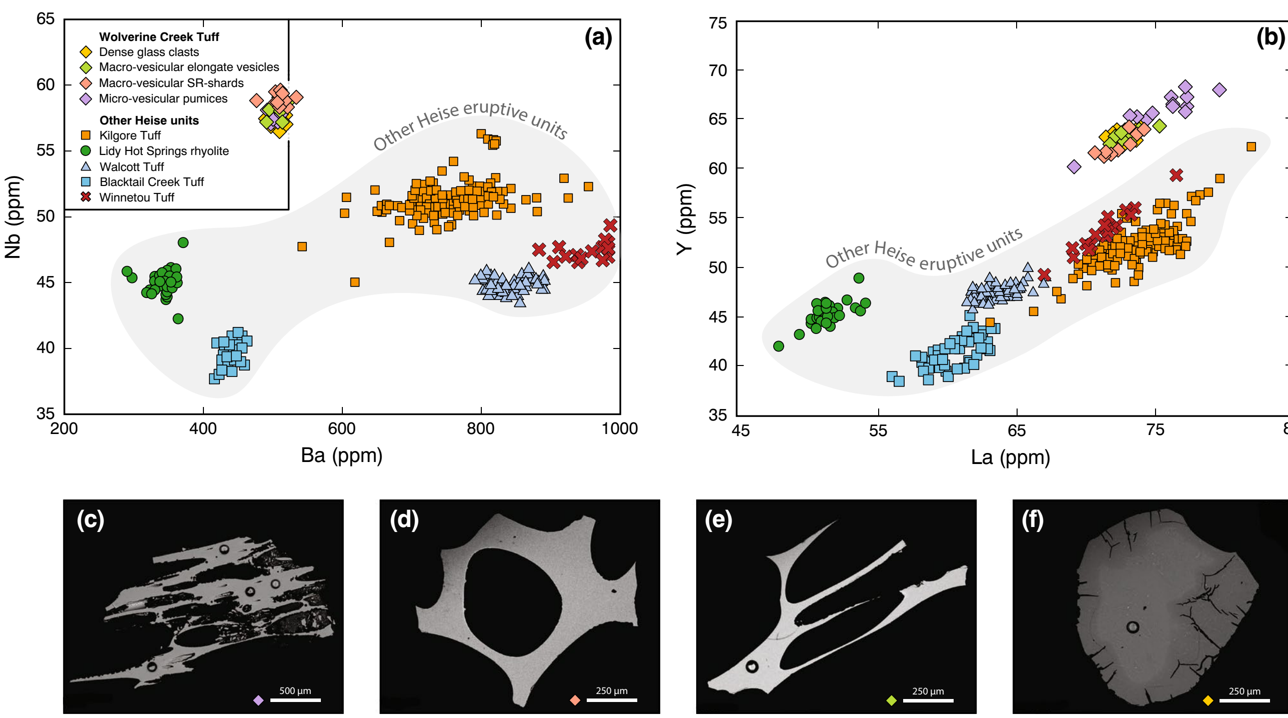

Fig. 5 Composition and appearance of obsidian clasts within the Wolverine Creek Tuff. **a**, **b** Trace elemental plots showing the compositions of WCT glasses with dense and vesicular glasses overlapping and distinguishing WCT from other Heise deposits (data from Ellis et al. 2017). **c**–**f** Appearance of the various glass morphologies in the WCT as described by Szymanowski et al. (2015), **c** microvesicular pumice, **d** classic SR-type macrovesicular shard, **e** macrovesicular shard with elongate vesicles, **f** dense obsidian clast showing a characteristically fractured and hydrated rim surrounding a brighter homogeneous core. Small circles in glasses represent pits for LA-ICPMS analyses

the element). The limited ability for major element geochemistry to distinguish between glass types is illustrated in Fig. 6 with respect to the Wolverine Creek case. When compared with Fig. 5, the difference in discriminating power between major and trace elements is clear.

Textural and compositional records

The three examples used in this study provide an overview of the major types of relationship between composition and texture preserved within dense glassy clasts from that deposit. Mesa Falls Tuff preserves a record of both textural and compositional heterogeneity where the obsidian clasts have a variety of origins (as illustrated by their compositions). This is consistent with the lack of relationship between the crystallinity and the composition of the obsidian. Cougar Point Tuff XIII contains a lot of textural variability within the obsidian clasts, but compositionally they are almost exclusively related to the juvenile component of the eruption. The Wolverine Creek Tuff has dense glass clasts that are both texturally homogeneous across the population (in the sense that they all share the hydrated rim and pristine interior) and are also geochemically similar. Thus, within a single deposit obsidian clasts of a single composition may be texturally variable, and there may be multiple, compositionally distinct sources of obsidians.

While we advocate the use of trace elemental fingerprinting for linking obsidian clasts with their co-erupted juvenile materials, this relies upon the geochemistry of the glass not be affected by later processes. The two main processes that can modify glass compositions are the post-eruptive crystallisation of the glass, and hydration. In the case of crystallisation, this may occur in relatively small regions

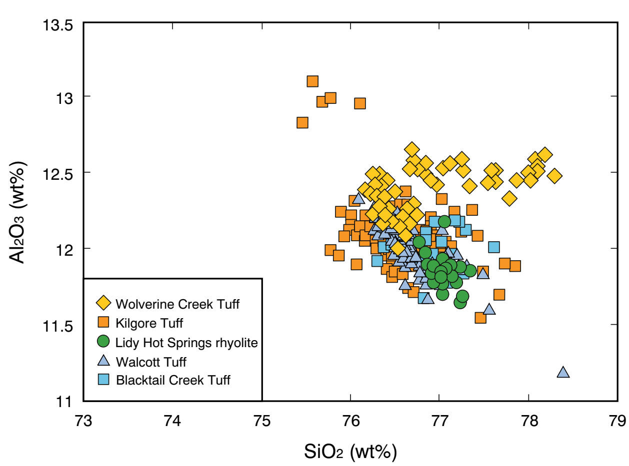

Fig. 6 Major elemental compositions of glasses from the Heise rhyolites (Ellis et al. 2017) highlighting the ability of trace elements (c.f. Figure 5) to discriminate eruptive events where major elements struggle

surrounding point sources such as spherulites or may be pervasive throughout the deposit with only small slivers of glass remaining. In the spherulite case, the geochemical perturbations are primarily observed close to the spherulite itself with far-field glass seemingly unaffected (Gardner et al. 2012). Where high proportions of the groundmass are crystallised, the effects on remaining portions of glass are, unsurprisingly, significant with incompatible elements such as Rb or Li markedly enriched in this remaining glass (Ellis et al. 2018). Particularly in the cases of the WCT and MFT deposits, any primary variability in the obsidians (e.g. microlite density) is overprinted by hydration rinds picked out by backscatter dark rims that are cut by fractures (Fig. 3c–d and Fig. 5f). It has long been recognised that hydration of silicic volcanic glasses can affect the geochemistry of the glass (Lipman et al. 1969; Cerling et al. 1985) and such effects have previously been reported in the Snake River Plain (Perkins et al. 1995). While hydration is not thought to affect the majority of trace elements, the abundances of the potentially affected elements (e.g. K, Na, Li) vary only slightly despite large textural differences (Fig. 7). This result is similar to the restricted compositional range reported in obsidians interpreted as juvenile from the Huckleberry Ridge Tuff (Swallow et al. 2018).

The origin of Snake River Plain obsidian clasts

Even allowing for the additional complexity imparted by pyroclastic transport and deposition, obsidian clasts appear to be near-ubiquitous in the products of explosive volcanism in the YSRP system. This argues for the obsidian clasts having a shared formation mechanism. While the Wolverine Creek obsidian clasts are generally similar in appearance to each other, the textural diversity in the mostly geochemically similar CPT XIII and Mesa Falls obsidian clasts is remarkable. Even considering the geochemical variability found within the MFT samples, the majority of the MFT obsidians have compositions akin to the juvenile component of the eruption (Fig. 3). Overall, from these case studies, particularly given the range of glass compositions produced from the same volcanic centres (Figs. 3, 4, and 5), we can conclude that the obsidians in the YSRP system are predominantly juvenile in origin (Fig. 8).

Previous studies (Branney et al. 2008; Ellis et al. 2010; Knott et al. 2016a, b) noted that the central Snake River Plain ignimbrites, while containing dense glassy clasts, lack either clasts of other, non-volcanic, lithologies or dense microcrystalline (or 'devitrified') rhyolite. Given that in the relatively distal regions where the ignimbrites are well-exposed the proportion of the deposits that are glassy is perhaps only 5–10%, this 'over-abundance' of dense glassy clasts requires explanation. The solution proposed in these studies was that the abundant glass was produced within

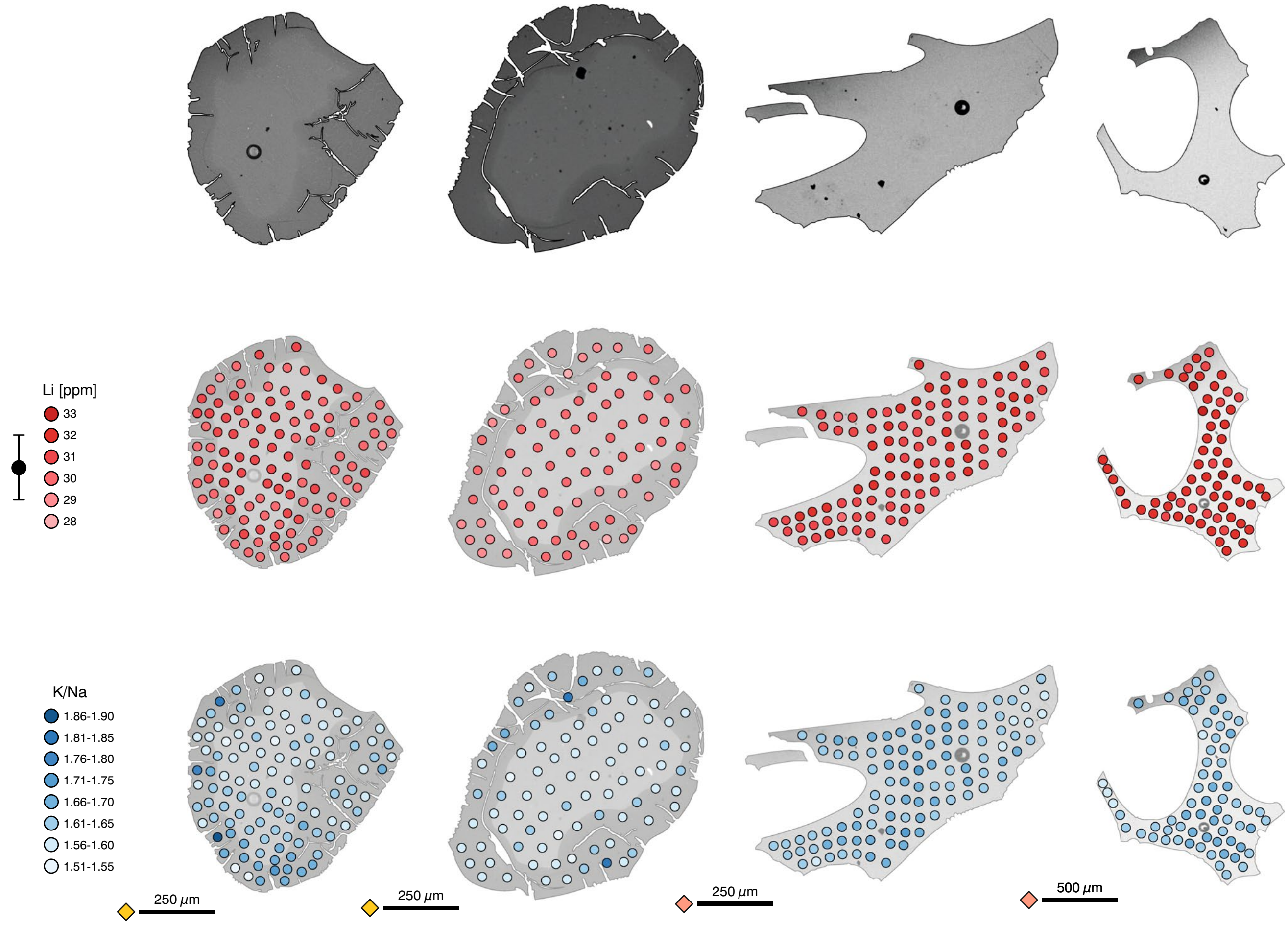

Fig. 7 Detailed analysis of Li, K, and Na abundances in microvesicular shards (salmon pink diamonds) and hydrated dense clasts (yellow diamonds) from the Wolverine Creek Tuff

the caldera from sub-aqueous effusions of magma forming hyaloclastite piles. This material was subsequently entrained in later eruptions that may have contained a (perhaps small) phreatomagmatic component. However, if hyaloclastites were being incorporated at source from potentially a few different effusive events, a much broader range of compositions might be expected. Additionally, only the Deadeye Member (which is entirely non-welded and contains abundant accretionary lapilli and mud clumps; Ellis and Branney 2010) provides any suggestion that it involved water-magma interaction during the eruption. The vast majority of the SRP ignimbrites are intensely welded (e.g. Figure 1), rather arguing for high depositional temperatures and where deposits are non-welded, such as in the Mesa Falls and Wolverine Creek cases, the juveniles are typically vesicular suggesting magmatic (rather than phreatomagmatic) fragmentation dominated.

With the compositional relations of the obsidian clasts revealed here, we prefer that they predominantly formed within the conduits and were subsequently evacuated as the eruption waxed (Fig. 8). This behaviour is increasingly recognised as mechanically complex (Kennedy et al. 2005) and may involve conduit filling material passing through many cycles of fragmentation and re-healing, which requires prolonged times at sufficient temperature (Gardner et al. 2019). Cougar Point Tuff XIII provides direct evidence for such processes as some of the obsidian clasts themselves contain smaller discrete clasts that are picked out by sharp boundaries and distinct changes in flow banding style and orientation (Fig. 9a). The coupled geochemical and phenocryst content data from the Mesa Falls Tuff provide additional support for such in-conduit processing from a different perspective (Fig. 9b). When the average compositions of each obsidian clast (from the multiple measurements per clast) are plotted along with their phenocryst content, it is clear that the crystallinity and the geochemical indicators of magmatic evolution are unrelated. If the physical and geochemical behaviour of the clasts were governed by crystallisation, it might be expected that in the most crystal-rich clasts the remaining

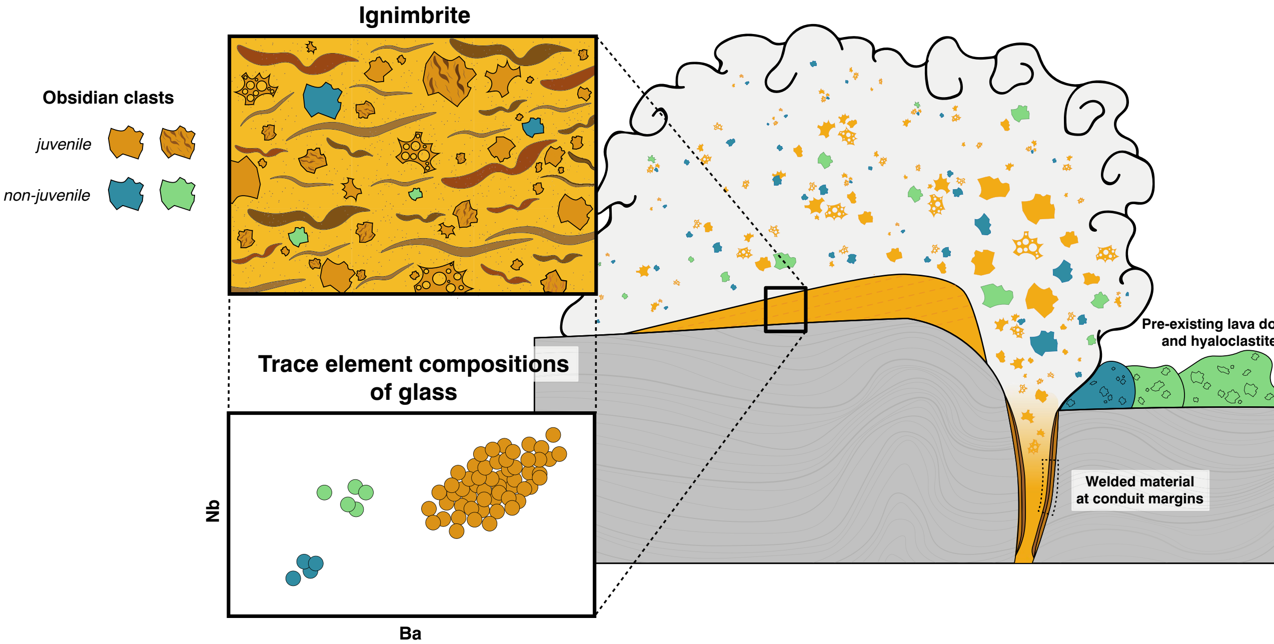

Fig. 8 Cartoon illustrating the potential origins for dense glassy clasts in pyroclastic deposits (dimensions not to scale). The lavas depicted within the caldera are coloured to represent glass compositions for that particular source. The YSRP ignimbrites have compositions indicating the dense glass cargos in these deposits are predominantly juvenile with likely scarce externally sourced obsidians

glass would be enriched in incompatible elements. The overall similarity in glass compositions at vastly different crystallinities may readily be explained by physical processes whereby melt of the same composition is mixed with different crystal components. The lack of hydration on rapidly quenched vesicular shards (Figs. 3 and 7) indicates that hydration did not happen post-deposition and thus the obsidian clasts must have inherited their texturally distinct rims elsewhere. We speculate that the rims on the obsidian clasts were formed within this vent environment prior to eruption where they experienced a temperature high enough to promote hydration but insufficient

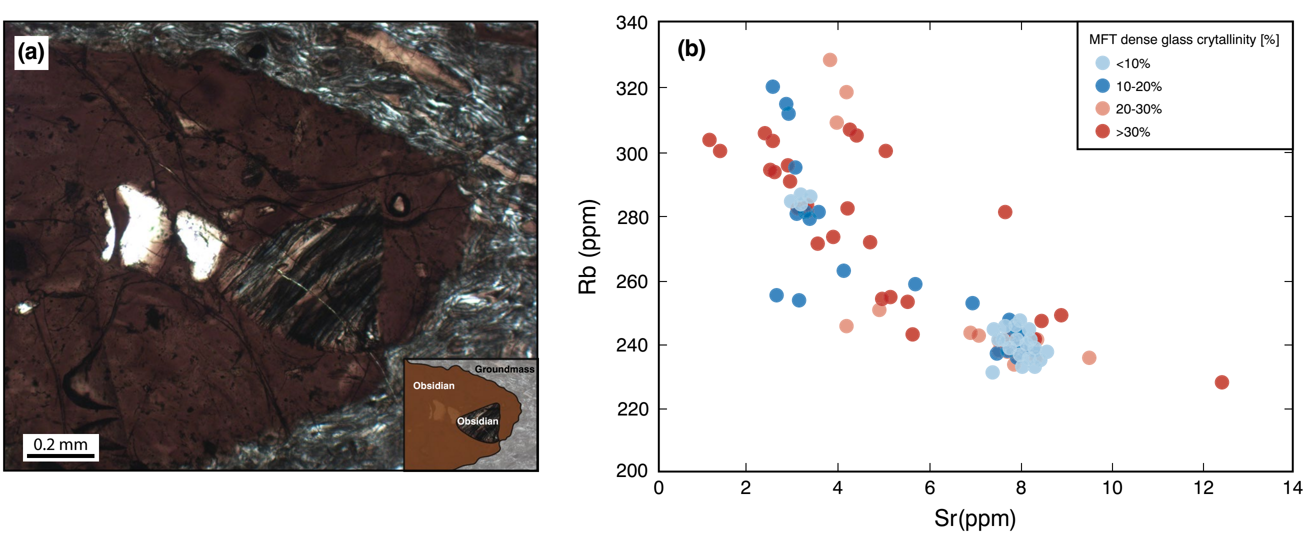

Fig. 9 Textural and geochemical support for a conduit origin for the YSRP obsidians. **a** Clast-within-clast texture in a CPT XIII obsidian, **b** geochemistry of MFT dense glassy clasts with fill reflecting the phenocryst content of the clast. The lack of relationship between crystal content and glass composition supports a role for physical mixing of components during repeated sintering and fragmenting in the conduit

to sinter the fragments back together (hydration exclusively on clast rims).

A notable feature of the Yellowstone-Snake River Plain province is that the geochemical kinship that predominates between obsidian clasts and vesicular juvenile particles exists in deposits that represent some of the largest known eruptions with volumes > 1000 km^3 DRE. The systematic geochemical relationship between dense obsidian clasts and vesiculated juveniles supports previous interpretations of these morphologies being related at smaller-volume eruptive centres (Newberry, Rust and Cashman 2007; Mono Craters, Newman et al. 1988) and hints at a similarity of process spanning eruptive volumes of several orders of magnitude.

Geochemical and physical complexity of magmatic systems

With this work, we highlight the ability of trace elemental geochemistry to genetically link the obsidian clasts with the vesiculated portions of the magma that erupted in the same event. However, we note that results have to be interpreted with due consideration for the complexity of the magmatic system. With increasingly sophisticated studies, it is clear that magmatic systems in the YSRP and beyond often contain multiple compositionally distinct melts that are erupted either synchronously or sequentially. From our results above, we interpret the majority of obsidian clasts in the YSRP ignimbrites to be related to the juvenile magma erupted, likely via early quenching onto conduit walls followed by later excavation during vent widening. In this interpretation, there is a likely temporal disconnect between the obsidian clasts and the juvenile material they are found deposited alongside. If the erupted melt composition changes over time, then the fingerprinting method we advocate here with trace elements may be fallible. A good example of such a situation is illustrated by Swallow et al. (2018) who report 4 compositionally distinct populations of obsidian clasts from the Huckleberry Ridge Tuff. These obsidians contain measurable CO_2 (indicating last equilibration at a pressure sufficient for rhyolitic melt to retain CO_2—i.e. at depth). While most of the obsidian clasts have compositional counterparts within the vesicular fallout material (Myers et al. 2016), one of the compositions of obsidians recognised within the fallout material is only found as vesiculated clast within the overlying ignimbrite. This suggests that the obsidian composition found in the Huckleberry Ridge Tuff fallout deposit was a ‘preview’ of a melt yet to be erupted as a vesicular component.

The mode of pyroclastic transport can further complicate the interpretation of obsidian clasts. Where the obsidians are found within fallout deposits, the potential sources are limited to the juvenile magma and the lithologies immediately surrounding the conduit. Where the obsidian clasts are found within ignimbrites, the parental pyroclastic density current may have entrained materials from the ground between the vent and the location of deposition, allowing for additional sources of obsidian. An outstanding example of this is within the Bishop Tuff (Hildreth 1979). Erupted from the Long Valley caldera system at 766.6 ± 0.4 ka (Mark et al. 2017), the Bishop Tuff represents a widespread pyroclastic deposit consisting of fallout and ignimbrite components with an estimated volume of 600–650 km^3 (Hildreth and Wilson 2007). The Bishop Tuff represents perhaps the best-studied explosive deposit on Earth (Hildreth 1979; Hildreth and Mahood 1986; Wilson and Hildreth 1997; Crowley et al. 2007 amongst many others), and this in-depth understanding of the deposit architecture is key to discriminating between populations of obsidian clasts that are found throughout the deposit. In the fallout deposits, flow-banded, partially vesiculated obsidian clasts are found and have been interpreted to reflect degassed juvenile magma initially welded in transient conduits and subsequently brought out as the eruption intensity waxed (Hildreth and Mahood 1986). Additionally, in the ignimbrite, there are abundant obsidian fragments that derive from the underlying Glass Mountain lava (Bailey 1976). Notably these fragments are restricted to certain sectors of the ignimbrite whereby the parental density current traversed a substrate of Glass Mountain lithology. This observation supports the origin of these obsidian clasts as lithics and highlights the importance of understanding the internal stratigraphy of the deposits.

Conclusions

The most important findings of our study are:

1) Unlike major elements that vary only slightly in rhyolitic glasses, trace elements have large compositional ranges and can reliably be used for distinguishing between the erupted products of different events from the same volcanic centre. This ability to compositionally ‘fingerprint’ the vesicular juvenile component of an eruption allows the origin of the commonly co-erupted dense obsidian clasts to be investigated. The large range of elements routinely measured by LA-ICPMS can ensure that the obsidian pyroclasts are indeed genetically related to the juvenile component of the eruption prior to further study of the obsidians that often focuses on volatile components (e.g. H_2O, δD, CO_2).
2) From our study, and comparison with literature data, the majority of the obsidian clasts in the Yellowstone-Snake River Plain ignimbrites have a juvenile origin. Likely these obsidians reflect material initially quenched along the caldera faults during the initiation of the eruption. Previous interpretations of the SRP-Y obsidian clasts

suggested they were eroded remnants of pre-existing intra-caldera lavas that produced abundant glass due to subaqueous emplacement. Given the differing glass trace element compositions observed between successive eruptions of a single centre, the origin by erosion of pre-existing domes appears subordinate.

3) The three case studies investigated here all have volumes from the hundreds to thousands of cubic kilometres (DRE), which along with data from the Huckleberry Ridge Tuff (Swallow et al. 2018; Girard and Stix 2010) indicates that the processes of obsidian generation within the conduit and subsequent erosion observed at smaller volume eruptions are also occurring during much larger events.

Supplementary Information The online version contains supplementary material available at https://doi.org/10.1007/s00445-021-01448-1.

Acknowledgements We would like to thank the editor, Alexei Ivanov, for efficient handling and Ulrich Küppers and one anonymous reviewer for thoughtful and constructive comments that helped us improve this paper.

Funding Open Access funding provided by ETH Zurich. This research was partially funded by Swiss National Science Foundation (200021_166281 to B.E.).

References

Andrews GDM, Branney MJ, Bonnichsen B, McCurry M (2008) Rhyolitic ignimbrites in the Rogerson Graben, southern Snake River Plain volcanic province: volcanic stratigraphy, eruption history and basin evolution. Bull Volcanol 70:269–291

Bailey RA (1976) Volcanism, structure, and geochronology of Long Valley Caldera, Mono County, California. J Geophys Res 81(5):725–744

Barnes JD, Prather TJ, Cisneros M, Befus K, Gardner JE, Larson TE (2014) Stable chlorine isotope behavior during volcanic degassing of H2O and CO2 at Mono Craters, CA. Bull Volcanol 76:805

Branney MJ, Bonnichsen B, Andrews GDM, Ellis B, Barry TL, McCurry M (2008) 'Snake River (SR)-type' volcanism at the Yellowstone hotspot track: distinctive products from unusual, high-temperature silicic super-eruptions. Bull Volcanol 70:293–314

Branney MJ, Kokelaar BP (2002) Pyroclastic density currents and the sedimentation of ignimbrites. Geol Soc Lond Mem 27:1–152

Cabrera A, Weinberg RF, Wright HMN, Zlotnik S, Cas RAF (2011) Melt fracturing and healing: a mechanism for degassing and origin of silicic obsidian. Geology 39(1):67–70

Cassidy M, Manga M, Cashman K, Bachmann O (2018) Controls on explosive-effusive volcanic eruption styles. Nat Commun 9

Castro JL, Bindeman IN, Tuffen H, Schipper CI (2014) Explosive origin of silicic lava: textural and δD–H2O evidence for pyroclastic degassing during rhyolite effusion. Earth Planet Sci Lett 405:52–61

Cerling TE, Brown FH, Bowman JR (1985) Low-temperature alteration of volcanic glass: hydration, Na, K, 18O and Ar mobility. ChemGeolIsotGeosci 52(3–4):281–293

Christiansen RL (2001) The Quaternary and Pliocene Yellowstone Plateau Volcanic Field of Wyoming, Idaho, and Montana. U. S. Geological Survey Professional Paper 729-G

Crowley JL, Schoene B, Bowring SA (2007) U-Pb dating of zircon in the Bishop Tuff at the millennial scale. Geology 35:1123–1126

Dunbar NW, Kyle PR (1992) Volatile contents of obsidian clasts in tephra from the Taupo Volcanic Zone, New Zealand: Implications to eruptive processes. J Volcanol Geoth Res 49(1–2):127–145

Ellis B, Branney MJ (2010) Silicic phreatomagmatism in the Snake River Plain: the Deadeye Member. Bull Volcanol 72:1241–1257

Ellis B, Szymanowski D, Wotzlaw JF, Schmitt AK, Bindeman IN, Troch J, Harris C, Bachmann O, Guillong M (2017) Post-caldera volcanism at the Heise volcanic field: implications for petrogenetic models. J Petrol 58(1):115–136

Ellis BS, Barry TL, Branney MJ, Wolff JA, Bindeman IN, Wilson R, Bonnichsen B (2010) Petrologic constraints on the development of a large-volume, high temperature, silicic magma system: the Twin Falls eruptive centre, central Snake River Plain. Lithos 120(3–4):475–489

Ellis BS, Schmitz MD, Hill M (2019) Reconstructing a Snake River Plain 'super-eruption' via compositional fingerprinting and high-precision U/Pb zircon geochronology. Contrib Miner Petrol 174:101

Ellis BS, Szymanowski D, Magna T, Neukampf J, Dohmen R, Bachmann O, Ulmer P, Guillong M (2018) Post-eruptive mobility of lithium in volcanic rocks. Nat Commun 9

Fink JH (1987) The Emplacement of Silicic Domes and Lava Flows. Geol Soc Am 212

Froggatt PC, Lowe DJ (1990) A review of late Quaternary silicic and some other tephra formations from New Zealand: their stratigraphy, nomenclature, distribution, volume, and age. NZ J Geol Geophys 33(1):89–109

Gardner JE, Befus KS, Watkins JM, Hesse M, Miller N (2012) Compositional gradients surrounding spherulites in obsidian and their relationship to spherulite growth and lava cooling. Bull Volcanol 74:1865–1879

Gardner JE, Llewellin EW, Watkins JM, Befus KS (2017) Formation of obsidian pyroclasts by sintering of ash particles in the volcanic conduit. Earth Planet Sci Lett 459:252–263

Gardner JE, Wadsworth FB, Llewellin EW, Watkins JM, Coumans JP (2019) Experimental constraints on the textures and origin of obsidian pyroclasts. Bull Volcanol

Girard G, Stix J (2010) Rapid extraction of discrete magma batches from a large differentiating magma chamber: the Central Plateau Member rhyolites, Yellowstone Caldera, Wyoming. Contrib Miner Petrol 160:441–465

Guillong M, Meier D, Allan M, Heinrich C, Yardley B (2008) SILLS: a MATLAB-based program for the reduction of laser ablation ICP-MS data of homogeneous materials and inclusions. Current Practices and Outstanding Issues. Mineralogical Association of Canada, Short Course Series . Vancouver:pp. 328–333

Hildreth W (1979) The BishopTuff: evidence for the origin of compositional zonation in silicic magma chambers. In: Chapin CE, Elston WE (eds) Ash-flow tuffs. Geol Soc Am Special Paper 180:43–75
Hildreth W, Mahood GA (1986) Ring-fracture eruption of the Bishop Tuff. Geol Soc Am Bull 97:396–403
Hildreth W, Wilson CJN (2007) Compositional zoning of the Bishop Tuff. J Petrol 48:951–999
Humphreys MCS, Menand T, Blundy JD, Klimm K (2008) Magma ascent rates in explosive eruptions: Constraints from H2O diffusion in melt inclusions. Earth Planet Sci Lett 270:25–40
Jollands MC, Ellis BS, Tollan PME, Müntener O (2020) An eruption chronometer based on experimentally determined H-Li and H-Na diffusion in quartz applied to the Bishop Tuff. Earth Planet Sci Lett 551
Kennedy B, Spieler O, Scheu B, Kueppers U, Taddeucci J, Dingwell DB (2005) Conduit implosion during Vulcanian eruptions. Geology 33(7):581–584
Knott TR, Branney MJ, Reichow MK, Finn DR, Coe RS, Storey M, Barfod D, McCurry M (2016a) Mid-Miocene record of large-scale Snake River–type explosive volcanism and associated subsidence on the Yellowstone hotspot track: The Cassia Formation of Idaho, USA. GSA Bull 128(7–8):1121–1146
Knott TR, Reichow MK, Branney MJ, Finn DR, Coe RS, Storey M, Bonnichsen B (2016b) Rheomorphic ignimbrites of the Rogerson Formation, central Snake River plain, USA: record of mid-Miocene rhyolitic explosive eruptions and associated crustal subsidence along the Yellowstone hotspot track. Bull Volcanol 78
Lipman PW, Christiansen RL, Van Alstine RE (1969) Retention of alkalis by calc-alkalic rhyolites during crystallization and hydration. Am Miner 54(1–2):286–291
Lloyd AS, Plank T, Ruprecht P, Hauri EH, William Rose W (2013) Volatile loss from melt inclusions in pyroclasts of differing sizes. Contrib Miner Petrol 165:129–153
Mark DF, Renne PR, Dymock RC, Smith VC, Simon JI, Morgan LE, Staff RA, Ellis BS, Pearce NJG (2017) High-precision 40Ar/39Ar dating of pleistocene tuffs and temporal anchoring of the Matuyama-Brunhes boundary. Quat Geochronol 39:1–23
McDonough WF, Sun S (1995) The composition of the Earth. Chem Geol 120(3–4):223–253
Moore LR, Gazel E, Tuohy R, Lloyd AS, Esposito R, Steele-MacInnis M, Hauri EH, Wallace PJ, Plank T, Bodnar RJ (2015) Bubbles matter: an assessment of the contribution of vapor bubbles to melt inclusion volatile budgets. Am Miner 100(4):806–823
Myers ML, Wallace PJ, Wilson CJN, Morter BK, Swallow EJ (2016) Prolonged ascent and episodic venting of discrete magma batches at the onset of the Huckleberry Ridge supereruption, Yellowstone. Earth Planet Sci Lett 451:285–297
Neukampf J, Ellis BS, Magnab T, Laurent O, Bachmann O (2019) Partitioning and isotopic fractionation of lithium in mineral phases of hot, dry rhyolites: the case of the Mesa Falls Tuff, Yellowstone. Chem Geol 506:175–186
Newman S, Epstein S, Stolper E (1988) Water, carbon dioxide, and hydrogen isotopes in glasses from the ca. 1340 A.D. eruption of the Mono Craters, California: constraints on degassing phenomena and initial volatile content. J VolcanolGeotherm Res 35(1–2):75–96
Perkins ME, Nash WP, Brown FH, Fleck RJ (1995) Fallout tuffs of Trapper Creek, Idaho—a record of Miocene explosive volcanism in the Snake River Plain volcanic province. GSA Bulletin 107(12):1484–1506
Portnyagin M, Almeev R, Matveev S, Holtz F (2008) Experimental evidence for rapid water exchange between melt inclusions in olivine and host magma. Earth Planet Sci Lett 272(3–4):541–552
Pritchard CJ, Larson PB (2012) Genesis of the post-caldera eastern Upper Basin Member rhyolites, Yellowstone, WY: from volcanic stratigraphy, geochemistry, and radiogenic isotope modeling. Contrib Miner Petrol 164:205–228
Queiroz G, Pacheco JM, Gaspar JL, Aspinall WP, Guest JE, Ferreira T (2008) The last 5000 years of activity at Sete Cidades volcano (São Miguel Island, Azores): implications for hazard assessment. J Volcanol Geoth Res 178:562–573
Rasmussen DJ, Plank TA, Wallace PJ, Newcombe ME, Lowenstern JB (2020) Vapor-bubble growth in olivine-hosted melt inclusions. Am Miner 105(12):1898–1919
Rust AC, Cashman KV (2007) Multiple origins of obsidian pyroclasts and implications for changes in the dynamics of the 1300 B.P. eruption of Newberry Volcano, USA. Bull Volcanol 69:825–845
Rust AC, Cashman KV, Wallace PJ (2004) Magma degassing buffered by vapor flow through brecciated conduit margins. Geology 32(4):349–352
Schipper CI, Castro JM, Kennedy BM, Tuffen H, Whattam J, Wadsworth FB, Paisley R, Fitzgerald RH, Rhodes E, Schaefer LN, Ashwell PA, Forte P, Seropian G, Alloway BV (2021) Silicic conduits as supersized tuffisites: clastogenic influences on shifting eruption styles at Cordón Caulle volcano (Chile). Bull Volcanol 83(11)
Shane P (2000) Tephrochronology: a New Zealand case study. Earth Sci Rev 49(1–4):223–259
Swallow EJ, Wilson CJN, Myers ML, Wallace PJ, Collins KS, Smith EGC (2018) Evacuation of multiple magma bodies and the onset of caldera collapse in a supereruption, captured in glass and mineral compositions. Contrib Mineral Petrol 173
Szymanowski D, Ellis BS, Bachmann O, Guillong M, Phillips WM (2015) Bridging basalts and rhyolites in the Yellowstone-Snake River Plain volcanic province: the elusive intermediate step. Earth Planet Sci Lett 415:80–89
Szymanowski D, Ellis BS, Wotzlaw JF, Buret Y, von Quadt A, Peytcheva I, Bindeman IN, Bachmann O (2016) Geochronological and isotopic records of crustal storage and assimilation in the Wolverine Creek–Conant Creek system, Heise eruptive centre, Snake River Plain. Contrib Mineral Petrol 171
Taylor BE, Eichelberger JC, Westrich HR (1983) Hydrogen isotopic evidence of rhyolitic magma degassing during shallow intrusion and eruption. Nature 306:541–545
Wadsworth FB, Llewellin EW, Vasseur J, Gardner JE, Tuffen H (2020) Explosive-effusive volcanic eruption transitions caused by sintering. Sci Adv 6
Wallace PJ, Kamenetsky VS, Cervantes P (2015) Melt inclusion CO2 contents, pressures of olivine crystallization, and the problem of shrinkage bubbles. Am Miner 100(4):787–794
Wang Y, Gardner JE, Hoblitt RP (2021) Formation of dense pyroclasts by sintering of ash particles during the preclimactic eruptions of Mt. Pinatubo in 1991. Bull Volcanol 83(6)
Waters LE, Lange RA (2015) An updated calibration of the plagioclase-liquid hygrometer-thermometer applicable to basalts through rhyolites. Am Miner 100(10):2172–2184
Watkins JM, Gardner JE, Befus KS (2017) Nonequilibrium degassing, regassing, and vapor fluxing in magmatic feeder systems. Geology 45:183–186
Wilson CJN, Hildreth W (1997) The Bishop Tuff: New Insights from Eruptive Stratigraphy. J Geol 105(4):407–440